Simple and Fast Decoding of Short LDPC Codes

Sahar Allahkaram*, Francisco A. Monteiro*, and Carlos Salema†
*Instituto de Telecomunicações, and ISCTE - Instituto Universitário de Lisboa, Portugal
†Instituto de Telecomunicações, and Instituto Superior Técnico, Universidade de Lisboa, Portugal
emails: {sahar.allahkaram, francisco.monteiro, carlos.salema}@lx.it.pt

***Abstract*—When using guessing random additive noise decoding (GRAND) to decode linear block codes (LBCs), the list of error patterns to be tested is blind to any structure in the parity-check matrix. This paper starts by proposing simple and general set partitioning (SP) constraints that reduce the number of possible patterns to less than half when decoding random linear codes (RLCs). Sparser parity-check matrices induce a faster decoding when using SP, but at the expense of a severe performance loss. This loss can be mostly recovered by considering regular or quasi-regular low-density parity-check (LDPC) codes. Given their structure, one can apply a simple constraint that, for given a syndrome, "filters" possible error positions. Subsequently, a guessing approach is applied to those few positions. The filtering threshold can be successively relaxed to extend the set of candidate positions. This technique alone reduces the average number of membership tests to $\simeq 5\%$ of the ones required by unconstrained GRAND, and often achieves near-to-one-shot decoding. Combined with SP, the number of membership tests drops to $\simeq 2\%$, leading to a maximum likelihood (ML) decoding of LDPC codes $50\times$ faster than unconstrained GRAND.**

***Index Terms*—Constrained GRAND, short codes, random linear codes (RLCs), LDPC codes, URLLC.**

I. Introduction

For error protection, binary messages with a length of k bits should be mapped to codewords n bits long, taken from a finite codebook $\mathcal{C}$, with a code rate $R = \frac{k}{n}$. Shannon showed that it is possible to communicate with an error probability that tends to zero when using a code with sufficiently long codewords ($n \to \infty$), as long as the code rate is below capacity [1]. When employing an error correction code (ECC), the asymptotic bit error probability (BER) decays as BER $\propto e^{-n\epsilon(R)}$, and, for large n, the error exponent is $\epsilon(R) \approx -\frac{\ln \mathrm{BER}}{n}$ [2]. The capacity corresponds to the highest code rate for which $\epsilon(R) > 0$. The statistics of the error exponent of random codes have been very recently analyzed in [3] when $n \to \infty$, proving that it converges to its expected value for both high and low code rates. Shannon's non-constructive proof showed that *random* codes could reach capacity [1], [4], [5], however, a simple maximum-likelihood (ML) decoder does not exist for such codes [6]. Decades-long research looked for codes capable of achieving capacity with some embedded *structure*, for which a feasible decoder could exist [7]. The focus was on reaching capacity, and the length of the codewords was not a major constraint. Low-density parity-check (LDPC) codes, also known as Gallager codes [8], later rediscovered by MacKay and Neal (MN) [9], [10], reach capacity for extremely large codewords.

Short codes became relevant for ultra-reliable low-latency communications (URLLC) [11], [12] in 6G [13], [14], even more than in 5G [15]. The capacity for the *finite* blocklength regime was found by Polyanskiy et al. [16], recovering Shannon's capacity when $n \to \infty$. The authors pointed out that very few prior works had looked at that problem, as considered by Salema [17, sec. 6.12-6.13], and by Dolinar et al. [18], who revisited Shannon's work considering finite codewords [2].

Ordered statistics decoding, which can be used to decode any LBC with quasi-ML performance [19], [20], has been proposed for short codes [21], [22]. Using a constrained serial list Viterbi algorithm, a very low number of codewords needs to be tested [23], however, this comes at the expense of a Gaussian elimination preprocessing for each received codeword, with a complexity that scales with $\approx \mathcal{O}(n^3)$.

High-speed decoding of LDPC codes (with $n = 1027$) has been presented in [24], which includes a list of other fast decoders implemented for n between 672 and 1994 bits. With a focus on fast decoding, short protographs LDPC codes have been proposed for URLLC, unfortunately enforcing rather resource-intensive very low code rates (from $\frac{1}{3}$ to $\frac{1}{12}$) [12].

Guessing random additive noise decoding (GRAND) is a *universal* ML decoder for codes with moderate redundancy. This includes short or high-rate random linear codes (RLCs), which attain the maximum possible rates of the finite blocklength regime [25]. GRAND-type decoders [26] where originally proposed by Duffy et al. as a hard ML decoder [11], [25], [27]. The concept shifted the decoding paradigm from finding the transmitted codeword to finding the error pattern that corrupted that codeword. This is done by successively testing error patterns in decreasing order of likelihood. In the case of RLCs, as for any linear block code (LBC), the membership test depends entirely on the observed syndrome [4], [26]. GRAND has been extended to soft-decoding [28], [29] and GRAND with joint detection has been analyzed in [30]. GRAND has been applied to fading channels in single-antenna [31] and multi-antenna systems [32]. GRAND has been implemented in hardware [33], [34] showing record energy-efficient decoding [35]. The noise-guessing concept has also been applied to network coding [36], to quantum ECCs [37] [38], and even to the purification of quantum links [39]. With GRAND, error-*detecting* codes, such as CRCs [40], or even the AES cryptosystem [41], can be turned into an ECC. GRAND can also compromise physical-layer security [42].

Although the statistics of the error patterns are central in determining the *order* in which they should be tested [11], [28], one should also restrict the *number* of possible error patterns that are worth testing. This was done in [43] by taking into account the modulation symbols. One can also take advantage of the parity-check matrix, $\mathbf{H}$. Given a syndrome, not all error patterns are compatible with the observed syndrome, which can greatly reduce the list of possible error patterns, $\mathcal{L}$.

Taking into account $\mathbf{H}$ and the observed syndrome, some constrained versions of GRAND have been proposed, achieving ML performance and requiring many fewer membership tests. In [44] constraints associated with the rows of $\mathbf{H}$ are used: for each considered row, the average number of tests is halved. However, processing those constraints becomes an extra burden, and the authors recommend using a single row. The work in [45] proposes splitting $\mathbf{H}$ in two matrices, one is used to generate low-weight error patterns via a (partial) trellis search and the other is used to check whether the candidate error patterns can generate the remaining partial syndrome. In [46] the idea is to start with a list of partial error patterns ordered in decreasing order of likelihood, as defined by the soft metrics of the bits, and complete the remaining error position by testing which position, associated with a column of $\mathbf{H}$, is compatible with the observed syndrome.

Short RLCs with GRAND have shown faster decoding than CRC-aided polar (CA-Polar) codes of similar length, or than standalone polar codes using the Tal-Vardy list decoder [28], [32], [47]. This paper starts by proposing simple constraints based on a set partitioning (SP) of the positions of the errors, which can be applied to *any* LBC, and is tested with RLCs. The existence of a very unbalanced number of ones and zeros in some row of $\mathbf{H}$ determines the reduction of complexity. Sparse RLCs would lead to faster decoding, however, at the expense of the codes' performance. By considering short LDPC codes, one can retain a good performance.

The second proposal in the paper applies to regular or quasi-regular LDPC codes, that is, codes with a sparse parity-check matrix with columns of equal weight. In the code's construction, we consider a relaxation of the conditions on the MN and Gallager codes [8]–[10] regarding column overlaps to randomly construct short LDPC codes. The proposed technique greatly reduces the number of positions involved in the guessing stage of the decoder, leading to a dramatic reduction of the average number of error patterns to be tested. A sieving mechanism is proposed to gradually increase the set of possible positions in which errors may have occurred.

The two techniques are eventually combined by applying SP to the reduced set of candidate positions coming from the filtering approach, which is accomplished with a simple intersection of position sets.

Notation: we use MATLAB's notation to denote rows and columns of a matrix: the i-th row is $\mathbf{H}(i,:)$ and the j-th column is $\mathbf{H}(:,j)$. The Hamming weight of a vector is denoted by its 1-norm, $||\cdot||_1$. A set of positions is denoted as $S=\{p_i\}, i=1,\ldots,|S|$. A set can be a set of positions (integers) or a set of binary vectors (error patterns). The addition in GF(2) is denoted by $\oplus$. The *overlap* between two binary column vectors is the number of common positions holding 1's.

II. Encoding schemes

A. Random Linear Codes: dense and sparse

A column vector $\mathbf{a}$ with k independent and identically distributed (i.i.d.) information bits is encoded by a LBC onto n-bits long codewords, $\mathbf{x}_{\mathrm{b}}$, and then mapped onto binary phase-shift keying (BPSK) or quadrature phase-shift keying (QPSK), subjected to additive white Gaussian noise (AWGN).

We start by considering short (systematic) RLCs, given their performance guarantees, mentioned in Section I. The elements of the generator matrix $\mathbf{G}\in\mathbb{F}_2^{n\times k}$ can be chosen uniformly at random from a Galois field $\mathbb{F}_q=\{0,1,\ldots,q-1\}$, where in this work, $q=2$. The $\mathbf{G}$ matrix defines a codebook $\mathcal{C}=\left\{\mathbf{x}_{\mathrm{b}}=\mathbf{G}\mathbf{a}:\mathbf{a}\in\mathbb{F}_2^k\right\}$ with $2^k=2^{nR}$ codewords of length n, which is a linear subspace of the discrete vector space $\mathbb{F}_2^n$. For systematic codes, $\mathbf{G}$ is of the form $\mathbf{G}=\left[\frac{\mathbf{P}}{\mathbf{I}_k}\right]$, where $\mathbf{P}\in\mathbb{F}_2^{(n-k)\times k}$ is a random binary matrix, whose elements have probabilities: $P(1)=p$ and $P(0)=1-p$. When $p=0.5$, we say that the RLC is dense, and for $p<0.5$ we say that the RLC is p-sparse. $\mathbf{I}_k$ is the $k\times k$ identity matrix associated with the systematic part of the encoding.

Any LBC can be also defined by the $(n-k)\times n$ parity-check matrix, $\mathbf{H}=[\mathbf{I}_{n-k}\,|\,\mathbf{P}_{(n-k)\times k}]\in\mathbb{F}_2^{(n-k)\times n}$, which spans the null space of $\mathbf{G}$, so that $\mathbf{HG}=\mathbf{0}$, and thus $\mathbf{H}\mathbf{x}_{\mathrm{b}}=\mathbf{0},\forall\mathbf{x}_{\mathrm{b}}\in\mathcal{C}$. A received block can be written as $\mathbf{y}_{\mathrm{b}}=\mathbf{x}_{\mathrm{b}}\oplus\mathbf{e}$, where $\mathbf{e}$ is the binary error vector after detection. The syndrome, $\mathbf{s}=[s_1,s_2,...,s_{(n-k)}]^T\in\mathbb{F}_2^{n-k}$, is computed as $\mathbf{s}=\mathbf{H}\mathbf{y}_{\mathrm{b}}=\mathbf{H}(\mathbf{x}_{\mathrm{b}}\oplus\mathbf{e})=\mathbf{He}$. GRAND uses the syndrome for the membership test, as $\mathbf{s}=\mathbf{0}$ only if $\mathbf{y}_{\mathrm{b}}\oplus\hat{\mathbf{e}}\in\mathcal{C}$, for some candidate error pattern $\hat{\mathbf{e}}$.

B. Quasi-regular LDPC codes with relaxed overlapping

Although short RLCs exist for any length and rate, the rules to design the parity-check matrices of MN codes and LDPC codes may not be feasible to fulfill for some desired lengths or rates. In its simplest form, a quasi-regular MN or LDPC code is constructed via its parity check matrix with two simple rules [9], [10]: 1) randomly generate different sparse columns for $\mathbf{H}$, all with equal weight w_c, 2) any new column, $\mathbf{h}_{\mathrm{new}}$, can only be allowed to have an overlap ≤ 1 with all previously accepted columns. The resulting code is a non-systematic one. To construct short LDPC codes we relax the second rule and tolerate overlaps ≤ 2. The overlaps can be easily checked by the inner product between columns of the extended $\mathbf{H}_{\mathrm{ext}}=[\mathbf{H}\,|\,\mathbf{h}_{\mathrm{new}}]$. The acceptance of a new column must check the off-diagonal elements of the Gram matrix: a new column $\mathbf{h}_{\mathrm{new}}$ is rejected if any element in $\mathbf{H}_{\mathrm{ext}}^T\mathbf{H}_{\mathrm{ext}}-w_c\mathbf{I}$ is >2.

As noted earlier, short RLC codes outperform short LDPC codes. However, for reasons that will become apparent in Section IV, having an $\mathbf{H}$ with equal column weights (quasi-regular LDPC codes), will allow to strongly reduce the number of candidate error positions. Regular LDPC codes would additionally have an equal weight, w_r, in all its rows, and could be used equally. Given its simpler construction, only quasi-regular codes will be considered.

III. Set partitioning for Linear Block Codes

We start by proposing the partition of the n positions of a received block $\mathbf{y}_\text{b}$ into sets. This allows to generate a shorter list of admissible error patterns, $\mathcal{L}$.

Definitions: the positions of the syndrome containing a 1 are called the *flagged positions* of the syndrome, and their number is $F = ||\mathbf{s}||_1$. In all of them, $\mathbf{s}(f) = 1$, for $f \in \{1, 2, \ldots, n-k\}$. The rows of $\mathbf{H}$ that are associated with these positions are called the *flagged rows*. The flagged rows are stacked to form the matrix $\mathbf{H}$-reduced, denoted as $\mathbf{H}_\text{red}$. The number of 1's in the i-th row of $\mathbf{H}$ is called the *support* of the row, and is denoted as supp$\{\mathbf{H}(i,:)\}$, as in [44]. Because $\mathbf{s} = \mathbf{He}$, we say that an error pattern $\mathbf{e}$ *activates* the j-th column of $\mathbf{H}$ when $e(j) = 1$. Each row of $\mathbf{H}$ has a *set of ones*, whose elements are the positions of the row that contain a 1, which is denoted as $\mathcal{S}_1$, and a *set of zeros*, which comprises the positions of the row holding a 0, which is denoted as $\mathcal{S}_0$. The sizes of these sets are, respectively, $|\mathcal{S}_1|$ and $|\mathcal{S}_0|$.

A. Construction of the admissible error sets

For a clearer explanation, we start by independently describing how the error patterns of weights $t = ||\mathbf{e}||_1 = 1, 2, 3$ are generated, and later we generalize to any even or odd weight.

1) One error case: In the case of a single error corrupting the block of n bits, there is no need to run membership tests by successively flipping single bits. Given that $\mathbf{s} = \mathbf{He}$, this situation corresponds to the case where only one column of $\mathbf{H}$ is active. This amounts to identifying whether the observed $\mathbf{s}$ is a copy of some column of $\mathbf{H}$. If only one error exists in position $p_1 = j$, then $\mathbf{s} = \mathbf{H}(:, j)$.

2) Two errors case: With two errors, any flagged position, f, in $\mathbf{s}$ can only result from two active columns $\mathbf{H}(:, p_1)$ and $\mathbf{H}(:, p_2)$, where the flagged row $\mathbf{H}(f,:)$ has in the positions $\mathbf{H}(f, p_1)$ and $\mathbf{H}(f, p_2)$ different bits. This means that the position of one of the errors must be in the *set of ones*, $\mathcal{S}_1$, of the row $\mathbf{H}(f,:)$ while the other error must necessarily be contained in the *set of zeros*, $\mathcal{S}_0$, of that same row.

The flagged rows are used to build the smaller matrix $\mathbf{H}_\text{red}$. The row of $\mathbf{H}_\text{red}$ that discloses more information about the location of the two errors is the one with the highest unbalance between the number of 0's and the number of 1's, i.e., the one where the sizes of the sets $\mathcal{S}_1$ and $\mathcal{S}_0$ that are most different. While the location of two errors among the n positions, all drawn from the same set, entails $|\mathcal{L}_2| = \binom{n}{2}$ possible error patterns, the list of all possible error patterns when the erroneous positions come from two disjoint sets is defined by the Cartesian product $\mathcal{S}_1 \times \mathcal{S}_0$, whose size is $|\mathcal{S}_1 \times \mathcal{S}_0| = |\mathcal{S}_1| \cdot |\mathcal{S}_0|$. Note that $\mathcal{S}_1 \times \mathcal{S}_0$ is a set of error patterns $\{\hat{\mathbf{e}}_1, \hat{\mathbf{e}}_2, \ldots, \hat{\mathbf{e}}_{|\mathcal{S}_1 \times \mathcal{S}_0|}\}$, where each error pattern is a set of positions, i.e., $\hat{\mathbf{e}}_i = \{p_1, p_2, \ldots, p_t\}$.

The number of candidate error patterns can be minimized by choosing the row of $\mathbf{H}_\text{red}$ that has the minimum support *or* the maximum support. From an information-theoretic perspective, that is the most informative row about the locations of the errors. The remaining entropy is subsequently dealt with by applying a noise-guessing approach that only considers the reduced set of candidate error patterns. The two extreme cases correspond to: a) $|\mathcal{S}_1| = 1$, where the number of error patterns with two errors is $|\mathcal{L}_2| = 1 \cdot (n-1)$, which is the case where $\mathcal{S}_1$ fully specifies the location of one of the two errors, leaving the other error position to be guessed among the remaining $n-1$ positions; b) $|\mathcal{S}_1| = |\mathcal{S}_0| = \frac{n}{2}$, leading to $|\mathcal{L}_2| = \frac{n}{2} \cdot \frac{n}{2} = \frac{n^2}{4}$. In benefit of the algorithmic complexity of the decoder, we opt for only looking at the row of $\mathbf{H}_\text{red}$ with the fewest 1's:

$$\mathbf{h}_m^T = \underset{1 \leq i \leq n-k}{\arg\min}\ \text{supp}\{\mathbf{H}_\text{red}(i,:)\}. \quad (1)$$

This option becomes optimal when sparse codes are considered, as $\mathbf{h}_m^T$ will always be the most unbalanced row.

In the case of $t = 2$, two other sets should also be formed: the *full set*, $\mathcal{F}$, which contains the positions p_j where the columns of $\mathbf{H}_\text{red}$ only have 1's (i.e., the columns of $\mathbf{H}_\text{red}$ with weight F), and the *null set*, $\mathcal{N}$, which contains the positions p_j where the columns of $\mathbf{H}_\text{red}$ are a zero vector. If one error $p_1 \in \mathcal{F}$, then it is easy to see that, necessarily, $p_2 \in \mathcal{N}$. Therefore, we have a new set of possible error patterns given by another Cartesian product: $\mathcal{F} \times \mathcal{N}$. Finally, the complete list of admissible error patterns is $\mathcal{L}_2 = (\mathcal{S}_1 \times \mathcal{S}_0) \cup (\mathcal{F} \times \mathcal{N})$, with size $|\mathcal{L}_2| = |\mathcal{S}_1| \cdot |\mathcal{S}_0| + |\mathcal{F}| \cdot |\mathcal{N}|$.

3) Three errors case: In the case of $t = 3$ errors, the flagged rows, and in particular the minimum support row, $\mathbf{h}_m^T$, can only trigger the flag if one of the two situations happens:

a) all three positions in error $p_1, p_2, p_3 \in |\mathcal{S}_1|$ and thus one has to search through all the possible error patterns with three positions in $\mathcal{S}_1$;
b) one error activated a 1 in the row and the other two lie "hidden" in the 0's, i.e., $p_1 \in \mathcal{S}_1$ and $p_2, p_3 \in \mathcal{S}_0$. Thus, one has to search through error patterns resulting from the Cartesian product of $\mathcal{S}_1 \times \mathcal{H}$, where $\mathcal{H}$ is the set of error patterns having all the combinations of two error positions "hidding" in $\mathcal{S}_0$.

With these constraints, the number of admissible error patterns with weight three is $|\mathcal{L}_3| = \binom{|\mathcal{S}_1|}{3} + |\mathcal{S}_1| \cdot \binom{|\mathcal{S}_0|}{2} \ll \binom{n}{3}$.

4) Any even or odd number of errors: Given that only an odd number of error positions in $\mathcal{S}_1$ can cause the syndrome flag associated with $\mathbf{h}_m^T$, when considering t errors, the set split is performed considering $2a + 1$ positions in $\mathcal{S}_1$, for $a \in \mathbb{Z}_0^+$ and $2a+1 \leq t$, and the remaining positions are errors "hidden" in $\mathcal{S}_0$. The cases detailed for $t = 1, 2, 3$ are particular examples of this simple rule. For simplicity, the full set and the null set are recommended to be used only in the $t = 2$ case. Without those two sets, in general, the total number of error patterns to be tested is:

$$|\mathcal{L}| = \sum_{i=0}^{t} |\mathcal{L}_i| = 1 + \sum_{i_\text{odd}}^{t} \binom{|\mathcal{S}_1|}{i_\text{odd}} \cdot \binom{|\mathcal{S}_0|}{t - i_\text{odd}} \ll \sum_{i=0}^{t} \binom{n}{i}. \quad (2)$$

IV. SIEVING GRAND FOR QUASI-REGULAR LDPC CODES

When the parity-check matrix is both sparse and all columns have equal Hamming weight, such as the ones of LDPC codes, the number of candidate error positions that need to be tested can be greatly reduced using a simple constraint (or "filter"), capable of gradually sieving candidate positions into a set, $\mathcal{P}$, with more positions being added to the set at different iterations. (See sieve algorithms for the closest vector problem in lattices [48], [49]). At each iteration, a GRAND approach only considers error patterns formed by error positions that belong to that reduced set of positions. We will next define that set and then explain the two proposed filtering mechanisms.

After the l-th iteration, the set is $\mathcal{P}^{(l)} = \{p_j\}$, containing the positions $p_j,\ j = 1, 2, \cdots, |\mathcal{P}^{(l)}|$. The size of the set increases monotonically, with more positions added to it in each iteration. The number of iterations is upper bounded by $w_c - 1$. When the algorithm reaches iteration $l = w_c - 1$ without finding the ML error pattern in any of the previous iterations, all the n positions will be in the set in that last iteration. After the first iteration, the set of candidate positions $\mathcal{P}^{(1)}$ is usually very small and, although $|\mathcal{P}^{(l)}|$ grows rapidly with each iteration, the number of error patterns to be tested for t errors in the l-th iteration is $\binom{|\mathcal{P}^{(l)}|}{t} \ll \binom{n}{t}$, for $k = 1, 2, \cdots, w_c - 1$. Note that the maximum number of iterations depends on the column weights of the LDPC code; nevertheless, the decoding can successfully terminate at a much earlier iteration if the ML $\hat{\mathbf{e}}$ has been found.

There are two mechanisms to reduce the number of error patterns: A) by looking at the weight of the syndrome and B) by filtering error positions, as described in the following.

A. Discarding error patterns by weight

By looking at the weight of the error syndrome, $||\mathbf{e}||_1$ it is possible to immediately discard some error patterns. For an $\mathbf{H}$ where all columns have constant weight w_c, the maximum weight of the syndrome can bear when t errors affect a codeword and is $\max\{||s||_1\} = t \cdot w_c$. This happens when all the 1's in the t activated columns of $\mathbf{H}$ are in disjoint rows, i.e., with none of them overlapping. When overlaps of columns $\mathbf{H}_{\text{red}}(:, j)$ take place, $||s||_1 \leq t \cdot w_c$. Therefore, when $||s||_1 > m \cdot w_c$, with $m \in \mathbb{Z}^+$, the decoder should only test error pattern with weights $||\hat{\mathbf{e}}||_1 > m$.

B. Filtering candidate error positions

We start by constructing $\mathbf{H}_{\text{red}} \in \mathbb{F}_2^{F \times n}$, consisting of the F flagged rows of $\mathbf{H}$, as defined in Section III. The sieving (or filtering) mechanism depends on the columns' Hamming weights: $\Sigma(j) = ||\mathbf{H}_{\text{red}}(:, j)||_1$, for $j = 1, \ldots n$. These weights can be simply computed by the sums $\sum_{i=1}^{F} \mathbf{H}_{\text{red}}(i, j)$, for $j = 1, \ldots n$, corresponding to the number of 1's in each column of $\mathbf{H}_{\text{red}}$. The iterations begin with an empty set of candidate positions $\mathcal{P}^{(0)} = \emptyset$. Next, more candidate positions are added such that $\mathcal{P}^{(1)} = \emptyset \cup \{p_i\}_{\text{new}}$. The mechanism for accepting positions into the candidate set is:

$$p_j \in \mathcal{P}^{(l)} \quad \text{if} \quad ||\mathbf{H}_{\text{red}}(:, j)||_1 \geq w_{th}(l), \tag{3}$$

where $w_{th}(l)$ is the value of a weight threshold during the l-th iteration, starting at $w_{th}(1) = w_c$. (While the number of possible positions is $|\mathcal{P}^{(l)}| < t$, w_{th} is lowered by one unit: $w_{th}(l+1) = w_{th}(l) - 1$.) At this point, the error patterns are tested running GRAND on the reduced set of positions $\mathcal{P}^{(l)}$, involving only $|\mathcal{L}| = \binom{|\mathcal{P}^{(l)}|}{t} \ll \binom{n}{t}$ candidate error patterns. The threshold is successively reduced in unit steps until the set of candidate positions $\mathcal{P}^{(l)}$ includes *all* the t positions where the errors lie, in which case the decoding of the ML error pattern $\hat{\mathbf{e}}$ will take place during the guessing stage.

For a visualization of these calculations, consider the following example:

$$\mathbf{H}_{\text{red}} = \begin{bmatrix}
0&1&0&0&0&0&0&0&0&1&0&0&0&0&1&0&0&0&1&0&0&0&0&0&1&1&0&0&0&0\\
0&0&0&1&0&1&0&0&0&1&0&0&0&0&0&0&0&0&1&0&0&0&0&0&0&0&0&0&0&1\\
0&1&1&0&1&0&0&0&0&0&1&0&0&0&0&0&1&0&1&0&0&1&1&0&0&0&0&0&1&0\\
0&0&0&0&0&0&1&0&0&0&0&0&1&0&0&0&0&0&0&0&0&0&0&1&0&0&0&0&0&1\\
0&1&1&0&0&1&0&0&1&0&0&1&0&0&0&0&1&0&0&0&0&0&1&0&0&0&0&1&0&0\\
0&0&0&0&0&1&0&0&0&0&0&0&0&0&0&0&0&1&0&0&1&0&1&1&0&0&0&1&0&1\\
0&0&0&0&0&0&0&1&0&1&0&1&0&0&0&1&0&1&0&0&1&0&0&0&0&0&1&0&0&1\\
0&1&0&0&1&0&1&1&0&1&1&0&0&1&0&0&0&0&0&0&0&0&0&0&0&0&0&0&0&0
\end{bmatrix}$$

$$\text{Sum} = \begin{bmatrix} 0&4&2&1&2&3&2&2&1&4&2&2&1&1&1&1&2&2&3&0&2&1&3&2&1&1&1&2&1&4 \end{bmatrix}$$

In this example, the different colors indicate the set of new positions that are added to the pool at each iteration. In the first iteration, the candidate positions are $\mathcal{P}^{(1)} = \{p_1, p_2, p_3\} = \{2, 10, 30\}$ (colored in blue), for the first threshold $w_{th}(1) = 4$. The set of candidate positions is subsequently extended to $\mathcal{P}^{(2)} = \{p_1, p_2, p_3, p_4, p_5\} = \{2, 6, 10, 19, 23, 30\}$ (colored in green), for $w_{th}(2) = 3$, and finally extended (if needed) to include the remaining positions where $||\mathbf{H}_{\text{red}}(:, j)||_1 \geq 2$ (colored orange).

Error patterns that have been tested in a previous iteration do not need to be re-tested after adding new positions to $\mathcal{P}$, as only error patterns that involve *new* positions added during each iteration need to be considered.

V. RESULTS

The system model described in Section II was numerically evaluated with RLCs (128,103), and an LDPC code (128,104) with $w_c = 4$ and $d_{\min} = 7$ (i.e., capable of correcting at least $t = 3$ errors), constructed as described in Subsection II-B, so that both systems have $R \approx 0.8$. For bit energy E_b and noise power spectral density N_0, we use the block error rate (BLER) as the performance metric, and the average number of error patterns tested as the complexity metric, both assessed as a function of E_b/N_0. In the case of RLCs, each transmitted message was assigned a randomly generated code so that the average performance of RLCs is measured. Let $t = 1, 2, 3$ be the maximum number of errors that a distance-bounded GRAND-based decoder aims to correct.

Fig.1 depicts the results using RLCs with set partitioning GRAND (SP-GRAND) compared to unconstrained GRAND. All BLERs are identical (all curves overlap) and the complexity curves show that SP-GRAND is substantially faster than unconstrained GRAND. For $t = 1$, only one membership check is needed, as seen in Section III-A1. For the more interesting $t = 2, 3$, SP-GRAND achieves 68% and 55% reductions if the average number of membership tests, respectively.

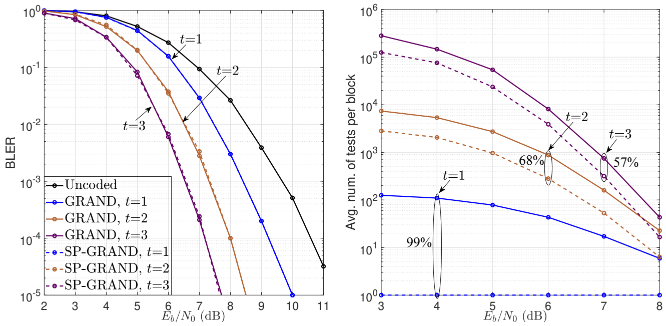

Fig. 1. BLER performance (left) and decoding complexity (right) for $t = 1, 2, 3$, using RLC (128,103) with set partitioning GRAND (SP-GRAND) compared with original GRAND.

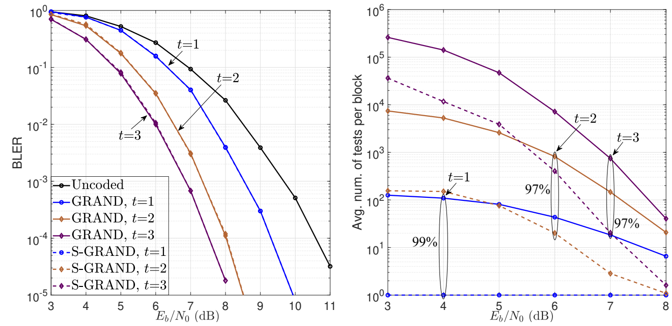

Fig. 2. BLER performance (left) and decoding complexity (right) for $t = 1, 2, 3$, using a LDPC code (128,104) with sieving GRAND (S-GRAND) compared with original GRAND.

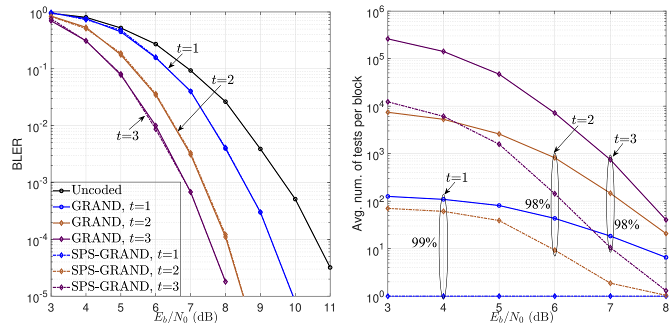

Fig. 3. BLER performance (left) and decoding complexity (right) for $t = 1, 2, 3$, using LDPC code (128,104) with combined set partitioning and sieving GRAND (SPS-GRAND) compared with original GRAND.

Fig.2 compares sieving GRAND (S-GRAND) and unconstrained GRAND for the LDPC code (128,104). The overlapping BLER curves confirm that S-GRAND attains ML decoding, given that all possible error patterns can eventually be tested. It is important to note that the RLCs outperform the similar-size LDPC code (comparing the left figures of Fig. 1 and Fig. 2). The 0.5 dB loss is due to the LDPC code itself rather than to the filtering mechanism applied in the decoding. The code's structure allows for much faster decoding, which is traded off by its slightly less good performance. As seen, the S-GRAND approach sharply reduces the number of membership tests needed by unconstrained GRAND, purging $\approx 97\%$ of the original $\sum_{i=0}^{t}\binom{n}{i}$ tests for $t = 2, 3$. This is achieved by considering a set of admissible error positions $\mathcal{P}^{(l)}$, of size $|\mathcal{P}^{(l)}| \ll n$, which includes the correct error positions with a monotonically increasing probability as the iterations unfold. Although in some cases, to find the ML $\hat{\mathbf{e}}$ the threshold has to be lowered down to $w_{th} = 2$, this happens with low probability, thus the average number of positions considered in the guessing stage remains consistently $\ll n$.

The SP and sieving techniques can be easily combined by applying SP to the candidate positions filtered at each iteration, leading to the here proposed set partitioning and sieving GRAND (SPS-GRAND). The resulting decoding of the LDPC code (128,104) is shown in Fig.3. As expected, SPS-GRAND has the same BLER as unconstrained GRAND. The complexity comparison reveals that SPS-GRAND outperforms GRAND outstandingly, eliminating on average over 98% of the membership tests, even when looking for $t = 3$ errors.

VI. Conclusion

This paper started by proposing a simple constraint for the decoding of any LBC. The constraint splits the positions of the errors into sets, allowing one to construct the error patterns by means of Cartesian between sets. With this set partitioning the complexity reduction is more accentuated with sparser codes. By using short quasi-regular LDPC codes, one can benefit from that without incurring a severe performance loss. For such codes, a simple filtering technique is used to greatly reduce the candidate positions where the error positions may lie. The technique is based on the "fingerprints" that the active columns of the parity-check matrix leave on the observed syndrome. This technique starts by selecting a small pool of positions where the errors most likely lie, and then GRAND runs on those few positions only. This is done iteratively, allowing more positions to be added to that pool until the ML error pattern is found. The number of these iterations is bounded by the weight of the columns of the parity-check matrix. The sieving approach finds the ML error pattern after testing on average only 5% of the original ones in unconstrained GRAND. The two techniques are entirely complementary and, when applied jointly, the complexity is reduced to about 2% of the original unconstrained GRAND.

Acknowledgments

This work has been funded by Instituto de Telecomunicações and FCT/MCTES (Portugal) through national funds and when applicable co-funded EU funds under the projects UIDB/50008/2020. Sahar Allahkaram is supported by a merit scholarship from ISCTE-IUL.

References

[1] C. E. Shannon, "A mathematical theory of communication," *The Bell Syst. Tech. J.*, vol. 27, no. 3, pp. 379–423, Jul. 1948.
[2] ——, "Probability of error for optimal codes in a gaussian channel," *The Bell Syst. Tech. J.*, vol. 38, no. 3, pp. 611–656, May 1959.
[3] L. V. Truong, G. Cocco, J. Font-Segura, and A. Guillén i Fàbregas, "Concentration properties of random codes," *IEEE Trans. Inf. Theory*, vol. 69, no. 12, pp. 7499–7537, Dec. 2023.

[4] D. J. C. MacKay, *Inf. Theory, Inference and Learning Algorithms*. Cambridge, UK: Cambridge Univ. Press, 2003.

[5] R. Gallager, “The random coding bound is tight for the average code (corresp.),” *IEEE Trans. Inf. Theory*, vol. 19, no. 2, p. 244–246, Mar 1973.

[6] J. Coffey and R. Goodman, “Any code of which we cannot think is good,” *IEEE Trans. Inf. Theory*, vol. 36, no. 6, pp. 1453–1461, Nov. 1990.

[7] D. J. Costello and G. D. Forney, “Channel coding: The road to channel capacity,” *Proc. of the IEEE*, vol. 95, no. 6, pp. 1150–1177, Jun. 2007.

[8] R. Gallager, “Low-density parity-check codes,” *IEEE Trans. Inf. Theory*, vol. 8, no. 1, pp. 21–28, Jan. 1962.

[9] D. MacKay and R. Neal, “Good codes based on very sparse matrices,” in *Cryptography and Coding 5th IMA Conf.*, ser. Lecture Notes in Computer Science, C. Boyd, Ed., no. 1025, 1995, pp. 100–111.

[10] D. MacKay, “Good error-correcting codes based on very sparse matrices,” *IEEE Trans. Inf. Theory*, vol. 45, no. 2, pp. 399–431, Mar. 1999.

[11] W. An, M. Médard, and K. R. Duffy, “Keep the bursts and ditch the interleavers,” *IEEE Trans. Commun.*, vol. 70, no. 6, pp. 3655–3667, Jun. 2022.

[12] X. Wu, M. Jiang, C. Zhao, L. Ma, and Y. Wei, “Low-rate PBRL-LDPC codes for URLLC in 5G,” *IEEE Wireless Commun. Lett.*, vol. 7, no. 5, pp. 800–803, Oct. 2018.

[13] C. Yue, V. Miloslavskaya, M. Shirvanimoghaddam, B. Vucetic, and Y. Li, “Efficient decoders for short block length codes in 6G URLLC,” *IEEE Commun. Mag.*, vol. 61, no. 4, pp. 84–90, Apr. 2023.

[14] M. Shirvanimoghaddam, M. S. Mohammadi, R. Abbas, A. Minja, C. Yue, B. Matuz, G. Han, Z. Lin, W. Liu, Y. Li, S. Johnson, and B. Vucetic, “Short block-length codes for ultra-reliable low latency communications,” *IEEE Commun. Mag.*, vol. 57, no. 2, pp. 130–137, Feb. 2019.

[15] K. Arora, J. Singh, and Y. S. Randhawa, “A survey on channel coding techniques for 5G wireless networks,” *Telecommun. Syst.*, vol. 73, no. 4, p. 637–663, Apr. 2020.

[16] Y. Polyanskiy, H. V. Poor, and S. Verdu, “Channel coding rate in the finite blocklength regime,” *IEEE Trans. Inf. Theory*, vol. 56, no. 5, pp. 2307–2359, May 2010.

[17] C. Salema, *Microwave Radio Links: From Theory to Design*. London, UK: Wiley, 2008.

[18] S. Dolinar, D. Divsalar, and F. Pollara, “Code performance as a function of block size,” TMO Progress Report, JPL-NASA, techreport 42-133, May 1998.

[19] M. Fossorier and S. Lin, “Soft-decision decoding of linear block codes based on ordered statistics,” *IEEE Trans. Inf. Theory*, vol. 41, no. 5, pp. 1379–1396, Sep. 1995.

[20] S. Alnawayseh and P. Loskot, “Ordered statistics-based list decoding techniques for linear binary block codes,” *EURASIP J. Wireless. Commun and Networking*, vol. 2012, no. 314, pp. 1–12, Oct. 2012.

[21] C. Kim, D. Kam, S. Kim, G. Park, and Y. Lee, “Simplified ordered statistic decoding for short-length linear block codes,” *IEEE Commun. Lett.*, vol. 26, no. 8, pp. 1720–1724, Aug. 2022.

[22] J. Liang, Y. Wang, S. Cai, and X. Ma, “A low-complexity ordered statistic decoding of short block codes,” *IEEE Commun. Lett.*, vol. 27, no. 2, pp. 400–403, Feb. 2023.

[23] Y. Wang, J. Liang, and X. Ma, “Local constraint-based ordered statistics decoding for short block codes,” in *2022 IEEE Inf. Theory Workshop (ITW)*, Mumbai, India, Nov. 2022, pp. 107–112.

[24] M. Li, V. Derudder, K. Bertrand, C. Desset, and A. Bourdoux, “High-speed LDPC decoders towards 1 Tb/s,” *IEEE Trans. Circuits Syst. I*, vol. 68, no. 5, pp. 2224–2233, May 2021.

[25] K. R. Duffy, J. Li, and M. Médard, “Capacity-achieving guessing random additive noise decoding,” *IEEE Trans. Inf. Theory*, vol. 65, no. 7, pp. 4023–4040, Jul. 2019.

[26] S. M. Abbas, M. Jalaleddine, and W. J. Gross, *Guessing Random Additive Noise Decoding: A Hardware Perspective*. Switzerland: Springer, 2023.

[27] K. R. Duffy, J. Li, and M. Médard, “Guessing noise, not code-words,” in *2018 IEEE Int. Symp on Inf. Theory (ISIT)*, Vail, CO, USA, Jun. 2018, pp. 671–675.

[28] K. R. Duffy, W. An, and M. Médard, “Ordered reliability bits guessing random additive noise decoding,” *IEEE Trans. Signal Process.*, vol. 70, pp. 4528–4542, Aug. 2022.

[29] S. M. Abbas, M. Jalaleddine, and W. J. Gross, “List-GRAND: A practical way to achieve maximum likelihood decoding,” *IEEE Trans. Very Large Scale Integration (VLSI) Syst.*, vol. 31, no. 1, pp. 43–54, Jan. 2023.

[30] H. Sarieddeen, P. Yuan, M. Médard, and K. R. Duffy, “Soft-input, soft-output joint data detection and GRAND: A performance and complexity analysis,” in *2023 IEEE Int. Symp on Inf. Theory (ISIT)*, Taipei, Taiwan, Jun. 2023, pp. 1090–1095.

[31] S. M. Abbas, M. Jalaleddine, and W. J. Gross, “GRAND for Rayleigh fading channels,” in *Proc. IEEE Globecom Workshops*, Rio de Janeiro, Brazil, Dec. 2022.

[32] S. Allahkaram, F. A. Monteiro, and I. Chatzigeorgiou, “URLLC with coded massive MIMO via random linear codes and GRAND,” in *IEEE 96th Vehic. Tech. Conf. (VTC2022-Fall)*, London, UK, Sep. 2022.

[33] A. Riaz, V. Bansal, A. Solomon, W. An, Q. Liu, K. Galligan, K. R. Duffy, M. Médard, and R. T. Yazicigil, “Multi-code multi-rate universal maximum likelihood decoder using GRAND,” in *Eur. Solid State Circuits. Conf. (ESSCIRC)*, Grenoble, France, Sep. 2021, pp. 239–246.

[34] C. Condo, “A fixed latency ORBGRAND decoder architecture with LUT-aided error-pattern scheduling,” *IEEE Trans. Circuits Syst. I*, vol. 69, no. 5, pp. 2203–2211, May 2022.

[35] A. Riaz, A. Yasar, F. Ercan, W. An, J. Ngo, K. Galligan, M. Médard, K. R. Duffy, and R. T. Yazicigil, “A sub-0.8pj/b 16.3gbps/mm2 universal soft-detection decoder using ORBGRAND in 40nm CMOS,” in *2023 IEEE Int. Solid-State Circuits Conf. (ISSCC)*, San Francisco, CA, USA, Feb. 2023, pp. 432–434.

[36] I. Chatzigeorgiou, “Transversal GRAND for network coded data,” in *2022 IEEE Int. Symp on Inf. Theory (ISIT)*, Espoo, Finland, Jun. 2022, pp. 1773–1778.

[37] D. Cruz, F. A. Monteiro, and B. C. Coutinho, “Quantum error correction via noise guessing decoding,” *IEEE Access*, vol. 11, Oct. 2023.

[38] D. Chandra, Z. B. Kaykac Egilmez, Y. Xiong, S. X. Ng, R. G. Maunder, and L. Hanzo, “Universal decoding of quantum stabilizer codes via classical guesswork,” *IEEE Access*, vol. 11, pp. 19 059–19 072, Feb. 2023.

[39] A. Roque, D. Cruz, F. A. Monteiro, and B. C. Coutinho, “Efficient entanglement purification based on noise guessing decoding,” *arXiv:2310.19914 [quant-ph] [cs.IT)]*, pp. 1–16, Oct. 2023. [Online]. Available: https://arxiv.org/abs/2310.19914

[40] W. An, M. Médard, and K. R. Duffy, “CRC codes as error correction codes,” in *IEEE Int. Conf. on Comm. (ICC)*, Montreal, QC, Canada, Jul. 2021, pp. 1–6.

[41] A. Cohen, R. G. L. D’Oliveira, K. R. Duffy, J. Woo, and M. Médard, “AES as error correction: Cryptosystems for reliable communication,” *IEEE Commun. Lett.*, vol. 27, no. 8, pp. 1964–1968, Aug. 2023.

[42] M. Médard and K. R. Duffy, “Physical layer insecurity,” in *57th Annual Conf. on Inf. Science and Syst. (CISS)*, Baltimore, MD, USA, Mar. 2023.

[43] I. Chatzigeorgiou and F. A. Monteiro, “Symbol-level GRAND for high-order modulation over block fading channels,” *IEEE Commun. Lett.*, vol. 27, no. 2, pp. 447–451, Feb 2023.

[44] M. Rowshan and J. Yuan, “Constrained error pattern generation for GRAND,” in *2022 IEEE Int. Symp on Inf. Theory (ISIT)*, Espoo, Finland, Jun. 2022, pp. 1767–1772.

[45] Y. Wang, J. Liang, and X. Ma, “Partially constrained GRAND of linear block codes,” *arXiv:2308.14259 [cs.IT]*, Aug. 2023. [Online]. Available: https://arxiv.org/abs/2308.14259

[46] R. Hadavian, X. Huang, D. Truhachev, K. El-Sankary, H. Ebrahimzad, and H. Najafi, “Ordered reliability direct error pattern testing decoding algorithm,” *arXiv:2310.12039 [cs.IT]*, Oct. 2023. [Online]. Available: https://arxiv.org/abs/2310.12039

[47] I. Tal and A. Vardy, “List decoding of polar codes,” *IEEE Trans. Inf. Theory*, vol. 61, no. 5, pp. 2213–2226, May 2015.

[48] F. Monteiro, “Lattices in MIMO spatial multiplexing: Detection and geometry,” Ph.D. dissertation, Univ. of Cambridge, UK, 2012.

[49] Z. Sun, C. Gu, and Y. Zheng, “A review of sieve algorithms in solving the shortest lattice vector problem,” *IEEE Access*, vol. 8, pp. 190 475–190 486, Oct. 2020.

APPENDIX

This Appendix offers additional comments and details regarding the two main proposals for set-splitting and sieving candidate positions.

We start by noting that the proposed decoder is a distance-bounded decoder, which does not try to decode beyond the number of errors t dictated by the minimum Hamming distance, d_{min}. Distance-bounded decoders do not reach capacity, with $n \to \infty$, as to reach capacity one has to be able to decode errors beyond $t = \frac{d_{\text{min}}-1}{2}$ [10] [4, Ch.13]. However, in the finite blocklength regime imposed in URLLC, this distinction has no practical meaning.

A. Distribution of the minimum support

The impact of splitting the n positions into the set of ones, $\mathcal{S}_1$, and the set of zeros, $\mathcal{S}_0$, depends on how low the weight of the minimum support row of $\mathbf{H}_{\text{red}}$ is. Therefore, it is important to look at the probability distribution of this weight $||\mathbf{h}_m^T||_1$, which corresponds to the size $|\mathcal{S}_1|$ in the minimum support row. The probability density function (PDF) of $|\mathcal{S}_1|$ is plotted in Fig. 4 for RLCs (128,103) with SP-GRAND. $P(|\mathcal{S}_1|)$ is a obviously a *discrete* variable. Its histogram was obtained via simulation and plotted as a continuous-variable approximation for easier visualization. Given that $\mathbf{H} = [\mathbf{I}_{n-k} \,|\, \mathbf{P}_{(n-k)\times k}] \in \mathbb{F}_2^{(n-k)\times n}$, dense RLCs (128,103) have on average 65 1s' in each row of $\mathbf{H}$: $\frac{n}{2}$ coming from the elements in the $\mathbf{P} \in \mathbb{F}_2^{(n-k)\times k}$ submatrix, plus one coming from the identity. The average weight of the minimum support row, $\mathbb{E}\{||\mathbf{h}_m^T||_1\} = \mathbb{E}\{|\mathcal{S}_1|\}$, must be lower than $\frac{n}{2}+1$. As observed in Fig. 4, the mean value $\mathbb{E}\{|\mathcal{S}_1|\} = 45$, and therefore $\mathbb{E}\{|\mathcal{S}_0|\} = n - \mathbb{E}\{|\mathcal{S}_1| = 83$. In this case, and considering $t = 3$, the number of possible error patterns is $|\mathcal{L}_3| = \binom{45}{3} + 45 \cdot \binom{83}{2} \ll \binom{128}{3}$.

Fig. 5 compares the number of error patterns required by unconstrained GRAND with the number of error patterns generated by the Cartesian products when set-partitioning is applied, considering different weights of the minimum support row, $|\mathcal{S}_1|$. The number of error patterns is plotted as a function of the codewords' length $2 \leq n \leq 128$, and in the case when one is trying to guess the locations of $t = 2$ errors. In the case of unconstrained GRAND (blue curve), the

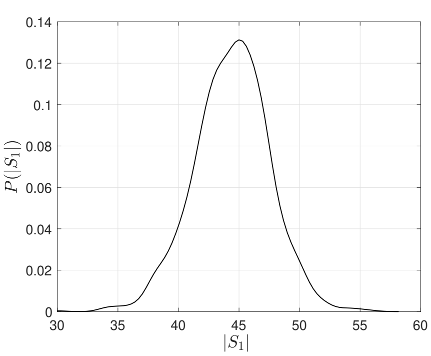

Fig. 4. PDF (continuous-variable approximation) for the number of 1's in the minimum support row of $\mathbf{H}_{\text{red}}$, using RLC (128,103).

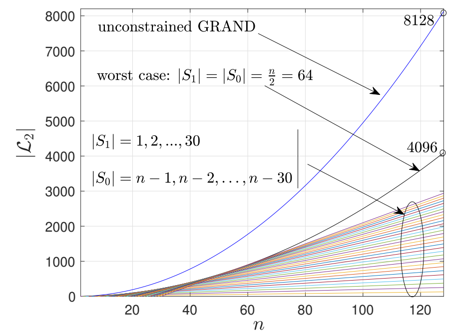

Fig. 5. Number of error patterns considered in unconstrained GRAND and in set-partitioning GRAND (SP-GRAND) for different weights of the minimum support row, $|\mathcal{S}_1|$, when looking for $t = 2$ errors.

number of error patterns is $|\mathcal{L}_2| = \binom{n}{2}$. When applying set-partitioning GRAND, the worst-case scenario (black curve) corresponds to the case where $|\mathcal{S}_1| = |\mathcal{S}_0| = \frac{n}{2}$, in which case $|\mathcal{L}_2| = \frac{n}{2} \cdot \frac{n}{2} = \frac{n^2}{4}$. This upper bound for SP-GRAND is always much lower than $\binom{n}{2}$. The figure also depicts several curves for a varying number of $|\mathcal{S}_1|$ and $|\mathcal{S}_0| = n - |\mathcal{S}_1|$ pairs. In all cases, $|\mathcal{L}_2| = |\mathcal{S}_1 \times \mathcal{S}_0| = |\mathcal{S}_1| \cdot |\mathcal{S}_0| \ll \binom{n}{2}$.

B. Distribution of $|\mathcal{P}^{(l)}|$ containing the t errors

The sieving approach adds at each iteration l a new set of positions to the set $\mathcal{P}^{(l-1)}$, leading to $\mathcal{P}^{(l)}$. A positive membership test takes place at the l-th iteration if and only if the correct t error positions $\{p_1, p_2, \ldots, p_t\} \in \mathcal{P}^{(l)}$. Fig. 6 shows the continuous-variable approximated PDF of the size $|\mathcal{P}^{(l)}|$ that contains *all* the $t = 3$ errors for an LDPC code (128,104) with the sieving decoder (S-GRAND). We get that the set sizes $|\mathcal{P}^{(l)}| \leq 10$ concentrate $\approx 74\%$ of the probability mass function (as seen in the cumulative distribution function (CDF) plotted in Fig. 6b). This very small pool of candidate positions translates into an extreme reduction of the average number of error patterns to be tested.

C. Distribution of the minimum support with positions filtering

After applying the filtering mechanism described in Section IV, the positions in the set $\mathcal{P}^{(l)}$ can be intersected with the ones in the $\mathcal{S}_1$ and $\mathcal{S}_0$ sets, resulting in the elimination of many of the positions in both $\mathcal{S}_1$ and $\mathcal{S}_0$. Fig. 7 depicts the continuous-variable approximated PDF of the number of positions in the intersection $|\mathcal{S}_1| \cap \mathcal{P}^{(l)}$, using the LDPC code (128,104), for $t = 3$. Compared with Fig. 4, where $\mathbb{E}\{|\mathcal{S}_1|\} = 45$, we now see in Fig. 7 that, when set partitioning and the sieving technique are applied simultaneously, $|\mathcal{S}_1|$ is always below 20 positions with probability 1.

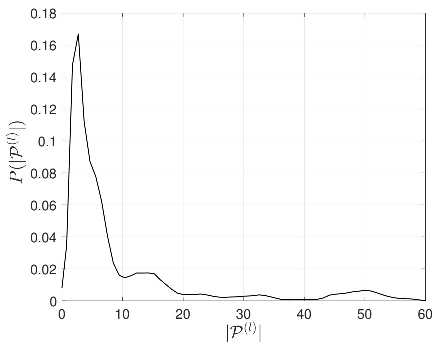

(a)

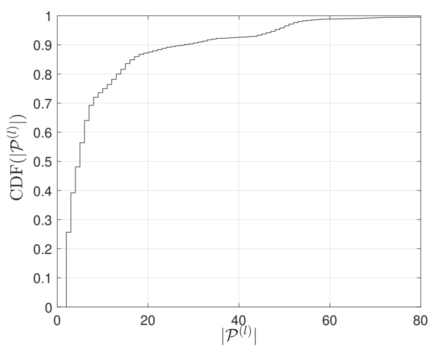

(b)

Fig. 6. PDF (continuous-variable approximation), and CDF, for the number of positions in the set $\mathcal{P}^{(l)}$ that contains all the t errors. The results are for the LDPC code (128,104), with the decoder searching for up to $t = 3$ errors.

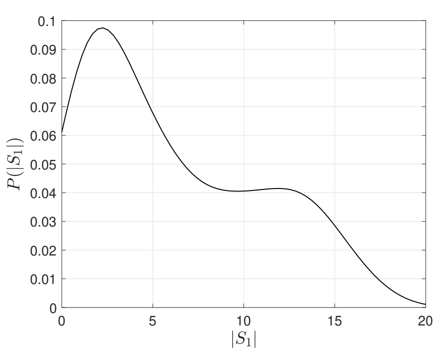

Fig. 7. PDF (continuous-variable approximation) for the number of all 1's in $\mathcal{P}^{(l)}$, after SPS-GRAND, using the LDPC code (128,104), with $t = 3$.

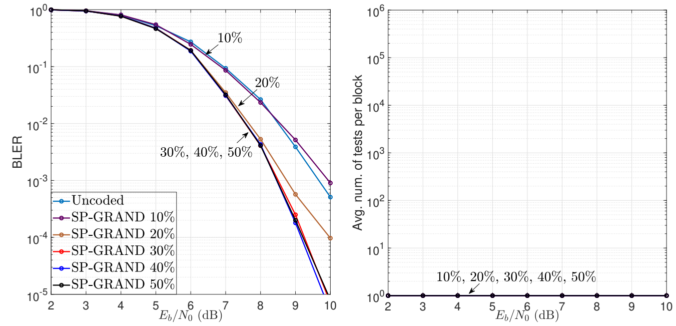

Fig. 8. BLER performance (left) and decoding complexity (right) for the number of error $t = 1$, using RLC (128,103) and BPSK, with p-sparse (indicated as a percentage) parity-check matrices, using set partitioning GRAND.

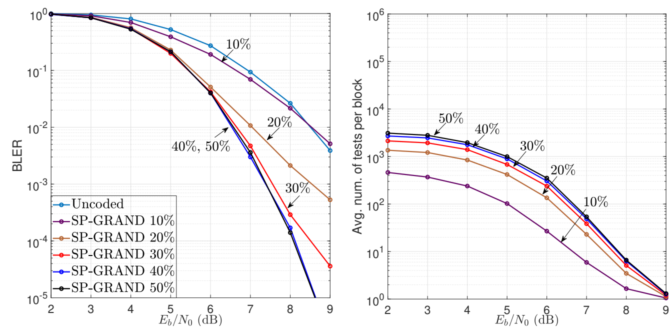

Fig. 9. BLER performance (left) and decoding complexity (right) for the number of errors $t = 2$, using RLC (128,103) and BPSK, with p-sparse (indicated as a percentage) parity-check matrices, using set partitioning GRAND.

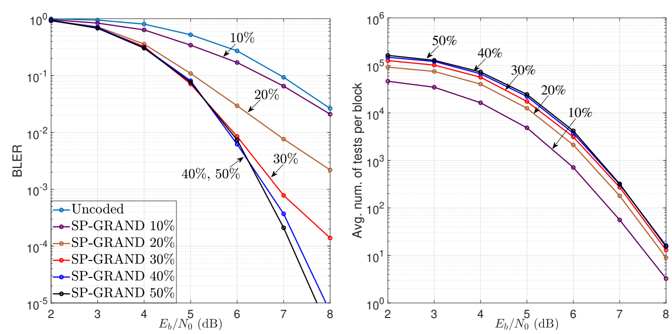

Fig. 10. BLER performance (left) and decoding complexity (right) for the number of errors $t = 3$, using RLC (128,103) and BPSK, with p-sparse (indicated as a percentage) parity-check matrices, using set partitioning GRAND.

D. Set partitioning GRAND with sparse RLCs

The number of candidate error patterns constructed via Cartesian products of two position sets gets smaller when the entropy of one of the sets is lower; fewer elements in a set provide more information about the errors' locations. Sparse RLCs, as defined in Section II-A necessarily verify the objective of having a low minimum support row $\mathbf{h}_m^T$. We assessed the performance and the complexity of SP-GRAND for RLCs (128, 103) with different sparsity values in their parity-check matrix, as shown in Fig. 8, Fig. 9 and Fig. 10 for bounded-decoders with $t = 1, 2, 3$, respectively. All figures include the performances of uncoded transmissions as well as the BLER and complexity results with SP-GRAND. With a sparser parity-check matrix, the weight of the minimum support row is lower and a faster decoding is possible, however, at the expense of a severe deterioration of the codes' performance, as one would expect (as they lack the proper construction of LDPC codes). It should be noted that the very sparse RLC codes can lead to a BLER even higher than the one of the uncoded transmission. This is because the added redundant bits contribute to more errors and the energy spent in their transmission is assigned to E_b, while this extra redundancy does not contribute to a codeword correction that compensates for that extra spent energy.

E. Sieving-GRAND technique

The technique proposed in Section IV for iteratively sieving candidate error positions, and also discarding error patterns by their weight, is presented in the flow chart in Fig. 11.

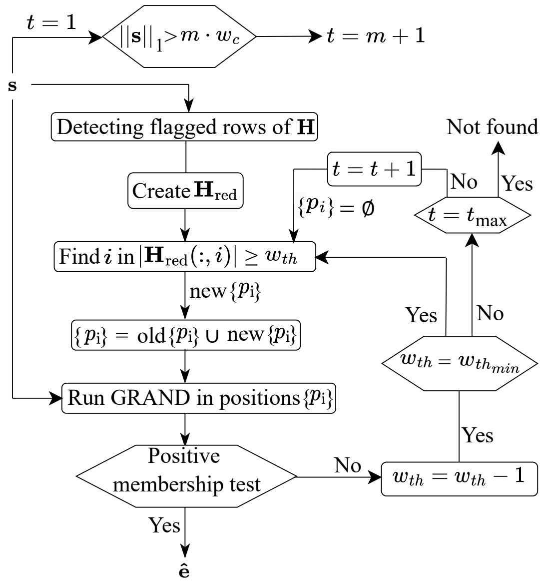

Fig. 11. Sieving (or filtering) candidate positions using i) a column weight threshold, and ii) the weight of the syndrome to discard error weights.

F. Mixing set partitioning and filtering

Here, a more detailed explanation of the filtering process is provided, followed by a more comprehensive explanation of how its combination with the set partitioning technique is implemented. To shed light on the concepts, an example with a very small parity-check matrix, with $n = 30$ and $n-k = 20$, will be discussed and illustrated bellow.

- Let us consider a number of flags in the syndrome $F = ||\mathbf{s}||_1 = 8$.
- both the *flags* and the *flagged rows* are highlighted by red arrows (rows $\{1, 3, 4, 5, 7, 9, 14, 16\}$).
- the flagged rows are stacked to form $\mathbf{H}_{\text{red}}$.
- the columns' Hamming weights are obtained: $\Sigma(j) = ||\mathbf{H}_{\text{red}}(:, j)||_1$, and the positions $\mathcal{P}^{(1)} = \{2, 10, 30\}$ are first selected, for a threshold $w_{th} = 4$ (colored blue), $\mathcal{P}^{(2)} = \{2, 6, 10, 19, 23, 30\}$, for $w_{th} = 3$ (colored green), and finally extended (if needed) to include the remaining positions where $||\mathbf{H}_{\text{red}}(:, j)||_1 \geq 2$ (colored orange).
- at this stage, the candidate error patterns are tested by running GRAND exclusively on a smaller subset of positions $|\mathcal{P}^{(l)}| = 6$ including only $|\mathcal{L}_t| = \binom{|\mathcal{P}^{(l)}|}{t} \ll \binom{n}{t}$ candidate error patterns. When looking for $t = 3$ errors, $|\mathcal{L}_3| = 20 \ll 4060$.

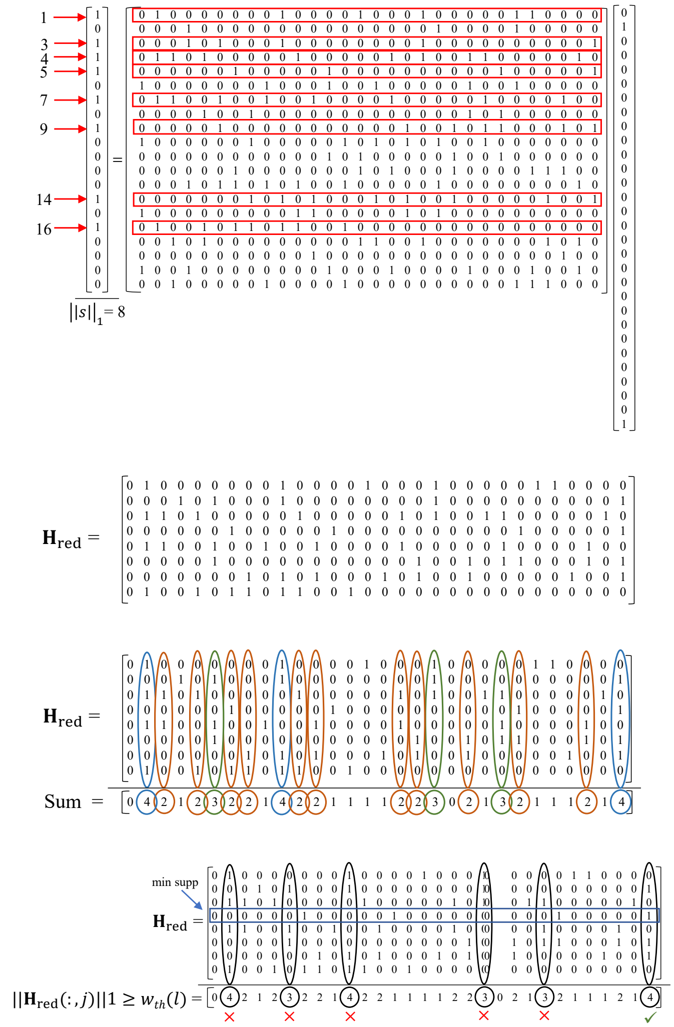

The simultaneous application of set partitioning and sieving techniques is exemplified at the end of the example above. It begins with $\mathcal{S}_1$ and $\mathcal{S}_0$, as defined by the minimum support row, and next, the set $\mathcal{P}^{(l)}$ intersects both $\mathcal{S}_1$ and $\mathcal{S}_0$. The admissible error patterns are generated by applying the sets partitioning technique while considering only the remaining positions in $\mathcal{P}^{(l)} \cap \mathcal{S}_1$ and $\mathcal{P}^{(l)} \cap \mathcal{S}_0$. In this example, $|\mathcal{P}^{(l)} \cap \mathcal{S}_1| = 1$, and $|\mathcal{P}^{(l)} \cap \mathcal{S}_0| = 5$. The number of candidate error patterns is $|\mathcal{L}_3| = 1 \times 5 \ll 4060$.

G. Results for a coded 16-QAM system

The proposed set partitioning and sieving GRAND (SPS-GRAND) operates at a bit level on the received LDPC codewords; nevertheless, the M-arity of the modulation modifies the performance of a coded system. Here, we present the BLER and complexity results when using the same coding schemes, now with 16-QAM (quadrature amplitude modulation; $M = 16$) with Gray mapping. The results are shown in Fig. 12, Fig. 13 and Fig.14, in the same order as in the main text. Fig.12 illustrates the performance and decoding complexity of RLC (128,103) using set partitioning GRAND

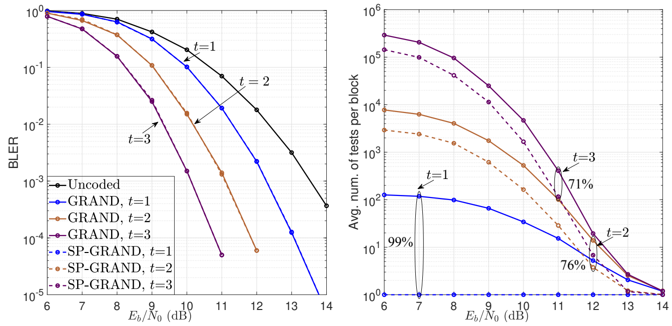

Fig. 12. BLER performance (left) and decoding complexity (right) for $t = 1, 2, 3$, using RLC (128,103) and 16-QAM, with set partitioning GRAND (SP-GRAND) compared with unconstrained GRAND.

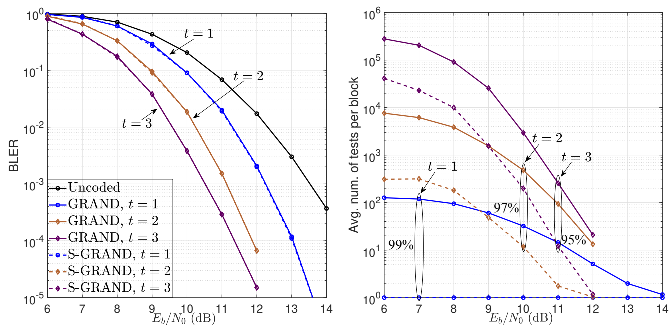

Fig. 13. BLER performance (left) and decoding complexity (right) for $t = 1, 2, 3$, using a LDPC code (128,104) and 16-QAM, with sieving GRAND (S-GRAND) compared with unconstrained GRAND.

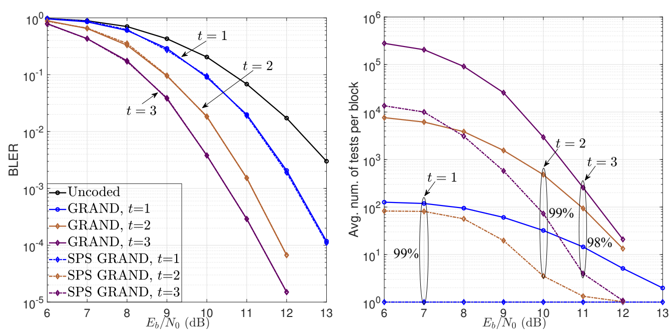

Fig. 14. BLER performance (left) and decoding complexity (right) for $t = 1, 2, 3$, using LDPC code (128,104) and 16-QAM, with combined set partitioning and sieving GRAND (SPS-GRAND) compared with unconstrained GRAND.

(SP-GRAND), in comparison to unconstrained GRAND. The BLER remains identical for SP-GRAND and unconstrained GRAND across the analyzed range of E_b/N_0, with the curves overlapping. As with $M = 2$ or $M = 4$ (BPSK or QPSK), with 16-QAM SP-GRAND also significantly reduces the number of tests needed with unconstrained GRAND: for $t = 2, 3$ the savings are over 70%. (In the case with $t = 1$, as seen in Section III-A1, only a direct comparison of $\mathbf{s}$ with all columns $\mathbf{H}(:, j)$ is needed, and only one membership test is involved.)

Fig.13 compares performances and decoding complexities of sieving GRAND (S-GRAND) and the original GRAND, when decoding the LDPC code (128,104). The BLER curves for both S-GRAND and GRAND perfectly overlap, indicating that in this setup S-GRAND also achieves the performance of ML decoding. As observed, S-GRAND significantly reduces the number of membership tests required by unconstrained GRAND, eliminating over 95% of the original $\sum_{i=0}^{t} \binom{n}{i}$ membership tests.

The decoded output of mixing set-partitioning GRAND and sieving GRAND for an LDPC code (128,104) is shown in Fig.14. As anticipated, within the specified E_b/N_0 range, SPS-GRAND holds the same BLER as unconstrained GRAND. Regarding complexity savings, the results also show the superiority of SPS-GRAND, ditching over 98% of the membership tests needed on average.